








Failure Modes and Reliability Oriented System Design for Aerospace Power Electronic Converters

JAYAKRISHNAN HARIKUMARAN ¹, GIAMPAOLO BUTICCHI ^{1,2} (Senior Member, IEEE),
GIOVANNI MIGLIAZZA ², VINCENZO MADONNA ¹ (Member, IEEE),
PAOLO GIANGRANDE ¹ (Senior Member, IEEE), ALESSANDRO COSTABEBER¹ (Member, IEEE),
PATRICK WHEELER ¹ (Fellow, IEEE), AND MICHAEL GALEA ^{1,2} (Senior Member, IEEE)

¹Power Electronics, Machines and Control Research Group, University of Nottingham, Nottingham NG7 2RD, U.K.

²Key Laboratory of More Electric Aircraft Technology of Zhejiang Province, University of Nottingham Ningbo China, Ningbo 315100, China

CORRESPONDING AUTHOR: JAYAKRISHNAN HARIKUMARAN (e-mail: Jayakrishnan.Harikumaran@nottingham.ac.uk).

This work was supported by the INNOVATIVE Doctoral Program, which is funded through the Marie Curie Initial Training Networks action under Grant 665468. This project also received funding from the Clean Sky 2 Joint Undertaking under the European Union's Horizon 2020 research and innovation programme under Grant Agreement 807081.

ABSTRACT Aircraft electrification has been a major trend in aviation industry for past 20 years. Given the increasing electrical power requirement for future more electric aircraft and hybrid electric aircraft, research efforts has been ongoing in high power electrical conversion for air-borne systems. Safety critical nature of aviation systems places reliability of aerospace power converters as a critical design concern. In this paper, power electronic system reliability is studied with emphasis on lifetime limiting factors of critical sub components. Reliability of voltage source power converters at different system voltage levels are modelled for a starter generator drive converter. A key observation is that Si IGBT devices are sufficient with respect to reliability requirements in low and medium voltage systems (up to 540 V). At higher system voltages (above 540 V), multi level topologies are necessary for designing with Si IGBTs. In constant power profile drive, system reliability is minimally affected by wear-out failure of film capacitors in converter DC links. In multi level topologies without enhanced voltage derating, system reliability is dominated by cosmic ray induced random failures. Simulation results demonstrate that at high system voltages (810 V), 2 L topology with SiC mosfets outperform Si IGBT based 3 L topology with respect to reliability.

INDEX TERMS Lifetime estimation, mission profile, more electric aircraft, multi level converter, physic of failure, reliability.

NOMENCLATURE

AEA	All electric aircraft
BVR	Blocking voltage ratio
DRAM	Dynamic random access memory
EMF	Electromotive Force
ESR	Effective series resistance
FIT	Failure in time
MEA	More electric aircraft
NPC	Neutral point clamped
NCEP	National Centers for Environmental Prediction
PCB	Printed circuit board

PoF	Physics of Failure
RBD	Reliability block diagram
SEB	Single event burnout
SEE	Single event error
SG	Starter Generator
2 L	Two Level
3L-NPC	Three Level Neutral Point Clamped

I. INTRODUCTION

The trend of greener and more energy responsible travel is resulting in an ever-increasing move towards transportation

electrification. In aviation, very challenging targets have been set by ACARE [1] with a target objective of achieving a net reduction of 75% in CO₂ emissions by 2050. MEA and AEA concepts have been proposed as means to reduce carbon intensity of aviation [2], [3].

In the MEA concept, aircraft subsystems, such as hydraulic and pneumatic air systems, are replaced with electrical counterparts. It is envisaged that electrically-driven subsystems could achieve an improved overall efficiency compared to conventional solutions. The MEA concept is being increasingly adopted by the aviation sector, which has resulted in a continuous upward trend in on-board power generation [4]. This trend will accelerate with the advent of the hybrid electric aircraft.

The core of the MEA system is the electric drive, which consists of - electric motors, power electronic converters, control platform and sensors [5]. In aerospace applications, electric drives must feature good efficiency along with a remarkable power density. The latter is obtained by pushing component performance, thus exposing them to considerable stresses - thermal, mechanical and environmental, which might compromise both component and system level reliability. Aerospace subsystems must meet very high reliability standards due to their safety critical nature. Hence in aerospace electric drives, reliability must be included as key design objective for simultaneously targeting the competing requirements of power density and reliability.

The main sources of failures in electric drive components include:

- 1) Electric motors - bearing failures, insulation failures;
- 2) Power electronic converter - semiconductor switches, capacitors, gate driver, PCBs etc [6];
- 3) Connection components - cables, connectors.

The main research focus of this work is on the reliability of power electronic converter and other components will not be considered. Traditionally, system reliability has been satisfied considering empirical safety margins derived from military handbooks at the design stage [7]. In recent years, however, there has been a progressive paradigm-shift, within both academia and industry, towards physics-of-failure - based design methodologies and assessments for power electronics converters [6]. These analyses are performed earlier in the design stages to feed into the detailed engineering phase of the converter system development. The analyses presented in this work try to fit in this research framework, by analysing and quantifying through a physics-based approach what are the most critical failure modes in typical power converters installed in an 'aerospace environment'.

Reliability analyses of power converters place emphasis on prominent failure prone power electronic components - semiconductor switches and capacitors [8]. The dominant wear-out failure mechanism in those components is thermal stress degradation [6]. Converters are subjected to dynamic stress profile in operation due to variations in environmental conditions and system operation. Mission profile based reliability studies have been reported in literature quantifying

component deterioration and system reliability for different power converter use cases, i.e., railway traction [9], electric vehicle [10], wind power [11] and aerospace [12].

Aerospace mission profile based reliability analysis of power converters is not widely available in literature. Furthermore, two important gaps exist in literature regarding reliability estimation of aerospace power converters.

- 1) Aircraft on-board power systems are evolving from the conventional 400 Hz AC grid [13] to HVDC distribution. In order to realize a light-weight electrical system, future aircraft power systems are expected to be designed for higher voltages with a possible DC grid. System voltage has a direct impact on component selection and consequently reliability estimation has to be performed at various voltage levels to give guidelines for system design choices.
- 2) Cosmic ray intensity at aircraft cruising altitudes is reported to be up to 300 times higher than that at sea level [14]. Impact of cosmic rays on semiconductors has been well established in literature and studied in detail for avionics (especially SEE leading to bit flips in DRAMs). Hence, as highlighted in [15], random failures due to cosmic rays must be included in reliability analysis for aerospace drive converters.

These gaps are addressed in a reliability case study for an aerospace drive application. Experimental loss measurement on a prototype converter is performed to validate loss estimation method employed in this work.

The main contributions of this paper are:

- 1) Wear-out failure lifetime estimation is combined with cosmic ray induced random failure rate estimation to account for aerospace mission profiles. It is shown that in high voltage systems (above 540 V) without enhanced voltage derating, cosmic ray induced failures is the reliability limiting factor in Si IGBT based converters.
- 2) The design choices considering reliability with respect to topologies (2 L or 3L-NPC) and devices (Si vs SiC) are illustrated as system voltage levels are varied. The results demonstrate that SiC devices are a suitable choice for future high voltage aerospace power converters. Multi level topologies must be employed to utilize Si IGBTs in order to meet reliability requirements.

II. FAILURE MECHANISMS AND LIFETIME MODELS IN POWER ELECTRONICS

A brief overview of major lifetime limiting factors of critical power electronic components and corresponding PoF-based lifetime models are provided. The PoF lifetime models illustrate the need for electro-thermal co-simulation for reliability modelling of power converters.

A. LIFETIME ESTIMATION OF SEMICONDUCTORS

1) WEAR-OUT FAILURE MECHANISMS IN SEMICONDUCTORS
During power converter operations, semiconductors experience cyclic power losses especially in electric drive due to the

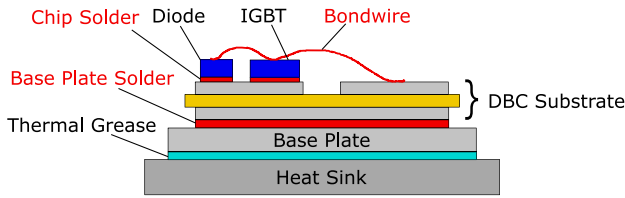


FIGURE 1. IGBT module cross section [16].

sinusoidal input or output waveforms. Repetitive power losses and consequent thermal cycles result in cyclic fatigue stresses in power modules as material properties (for instance, coefficient of thermal expansion) of semiconductor substrate, insulators and base plate metal are different [16]. Mean junction temperature of semiconductor also leads to thermal ageing by chemical processes [6], [17].

The key lifetime limiting sub-components in a power module are marked in red in Fig. 1. The most comprehensive lifetime model for power modules is given by Infineon named after Prof. Bayerer [18]. The model accounts for thermal stresses as well as module specific characteristics. Semikron power semiconductor manual lists the lifetime model as reproduced in (1), where N_f is module lifetime in number of thermal cycles when subjected to thermal cycles of magnitude δT_j with minimum junction temperature $T_{j,\min}$ during the thermal cycle with cycle heating time t_{on} . A is a curve fitting constant, I_B is current per bond wire, V_C is the voltage class of the module and D is the bond wire diameter in μm .

$$r \ln N_f = A \cdot \Delta T_j^{\beta_1} \cdot \exp\left[\frac{\beta_2}{T_{j,\min}}\right] \cdot t_{on}^{\beta_3} \cdot I_B^{\beta_4} \cdot V_C^{\beta_5} \cdot D^{\beta_6} \quad (1)$$

The model parameters applicable to a wide range of modules are summarized as $A = 9.34E14$; $\beta_1 = -4.416$; $\beta_2 = 1285$; $\beta_3 = -0.463$; $\beta_4 = -0.716$; $\beta_5 = -0.761$; $\beta_6 = -0.5$. The validity range of sub terms of the lifetime model is also provided in [16]. This limitations would be addressed in a later section. Lifetime models and parameters for SiC modules are not widely available in literature. One of the available lifetime studies on SiC devices highlight lower lifetime figures of SiC modules compared to Si [19]. The above work concludes that as the Young's Modulus of SiC material is higher than Si, the solder layer in a SiC module experiences higher fatigue stresses than in a Si module for the same junction temperature profile. The published results are valid in the temperature swing range of [90–140] °C. The lifetime model parameter is updated to $A = 4.67E14$ based on the results from [19] to reflect the increased thermal fatigue in SiC modules. An additional lifetime estimate is carried out to present the variation in lifetime estimates.

The mission profile based reliability estimation methodology considering wear-out failures of IGBTs is summarized in Fig. 2.

This is a widely adopted methodology in previous lifetime modelling studies considering only wear-out failures [20]. Particular attention was paid to device thermal modelling.

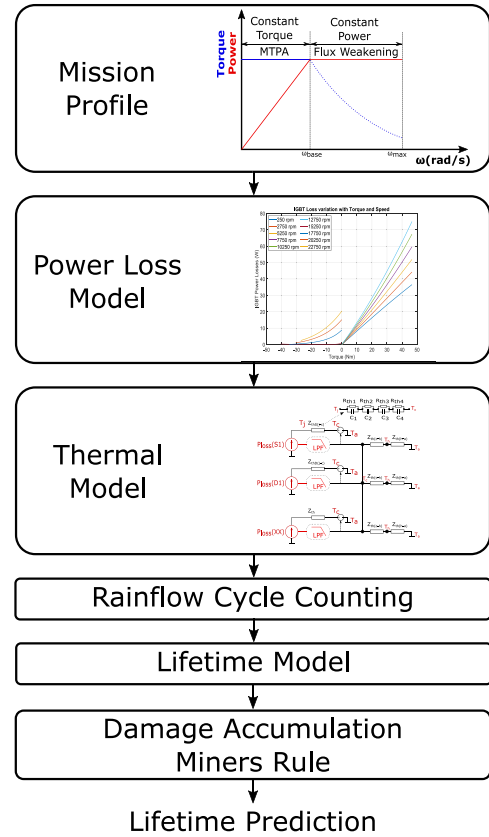


FIGURE 2. Mission profile based reliability estimation methodology for IGBTs.

Direct connection of Foster networks ignores the effect of thermal capacitance leading to erroneous estimation of junction temperature profile. An accurate approach of modelling thermal impedance has been proposed in [21] and has been adopted.

2) COSMIC RAY INDUCED RANDOM FAILURES IN SEMICONDUCTORS

Highly energetic atomic particles and ions are generated in the earth's atmosphere due to cosmic radiation. These particles, upon collision with atoms in semiconductor bulk, cause nuclear reactions. The fission products of nuclear reactions deposit a charge in semiconductor bulk. Thus, the high electric field present during reverse blocking mode (as shown in Fig. 3) could result in development of a streamer of electrons and holes that might lead to a sudden device destruction, due to short circuiting of a phase leg [22], [23].

The main factors influencing cosmic ray failure rate are reverse blocking voltage as well as particle flux intensity with sufficient energy. Emphasis is placed on atmospheric neutron intensity as it is the main contributor to cosmic ray failures in earth's atmosphere [24]. Cosmic ray failure is a complex physical phenomena and hence generalized failure models are not available. An analytical failure model for few specific

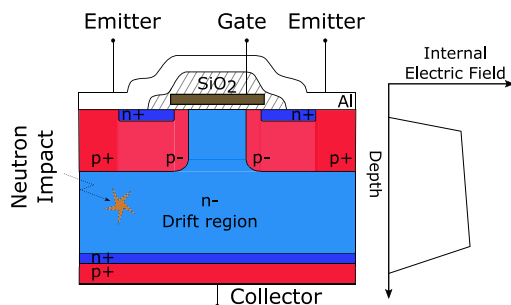


FIGURE 3. IGBT Cross section and internal electric field in blocking mode.

modules considering blocking voltage, junction temperature and atmospheric altitude was proposed in [25].

The IEC standard 62396-4 specifically addresses SEB in high voltage power devices for aircraft applications [26]. According to IEC62396, the neutron flux density at any point in the atmosphere could be obtained by scaling the value given at a reference location specified by its latitude, longitude and altitude. A neutron flux of $6000 /cm^2 h$ is reported for neutrons with energy $> 10 MeV$ at an altitude of 40000 ft at 45° latitude [27]. The above value is recommended by IEC 62396 to evaluate SEB failure rate. The estimation procedure outlined in [26] relies on experimental measurement of cosmic ray failure rate during exposure to reference neutron flux intensity.

IEC recommendations are adopted in this work to predict cosmic ray failure rate from experimentally reported failure rates for selected modules [28], [29]. The failure rate figures are scaled to account for altitude dependent flux intensity variation.

B. LIFETIME ESTIMATION OF CAPACITORS

Reliability analysis of capacitors for power electronics has been performed based on the well known Arrhenius degradation model [30], [31]. Along with temperature, applied voltage and humidity adversely affect capacitor lifetime [30]. The effect of humidity is ignored in this work as hermetic sealing of capacitors is assumed. A lifetime model addressing effects of temperature and voltage is provided in (2), where L is the capacitor lifetime under test conditions (hot spot temperature T and applied voltage U), while L_0 , T_0 and U_0 are lifetime, hot spot temperature and applied voltage at reference conditions [32]. E_a is the activation energy term, k_b is Boltzmann constant and β is a curve fitting term based on device technology. This study assumes dc link capacitors being composed of film capacitors as is the norm for high reliability applications. Lifetime model (2) is chosen as it is proposed for film capacitors.

$$rL = L_0 \cdot \exp^{\frac{E_a}{k_b} \left(\frac{1}{T} - \frac{1}{T_0} \right)} \cdot \exp^{-\beta \left(\frac{U-U_0}{U_0} \right)} \quad (2)$$

In the presented investigation these values are adopted: $L_0 = 1E5$ hours; $T_0 = 70^\circ C$; $\beta = 3.5$; $E_a = 9.891E-20$; $U_0 =$ rated voltage of the capacitor under study. A key distinction is drawn to the attention of readers that, the

TABLE 1. Starter Generator Parameters

Maximum Power	45 kW
Phase and pole numbers	3 phase, 6 pole
Maximum mechanical speed	32000 rpm
Stator resistance	1.1 m Ω
d-axis, q-axis inductance	99 μH
Back EMF constant, K_e	0.0259 V·s/rad

lifetime model predicts an increase in lifetime as operational temperature is reduced. In the case of aerospace applications, the ambient temperatures can reach $-50^\circ C$ or lower. The predicted lifetime figures would be unreasonably high. There are very few prior works in literature which reports capacitor lifetime at low temperatures. It was reported in [33] that film capacitors show very little degradation in electrical parameters at low temperatures. A clear guideline on capacitor lifetime modelling at low temperatures is stated in IEC 61709 [34]. The standard specifies usage of a constant failure rate for capacitors based on expected lifetime at $25^\circ C$. In this, capacitor temperature is saturated at $25^\circ C$ for reliability assessment.

III. CASE STUDY OF SG DRIVE CONVERTER

A simulation case study of a SG drive system is presented to illustrate the consequences of topology and device selection on system reliability. Switching over voltage and DC link voltage ripple has not been accounted for in the case study.

Reliability estimation is carried out in the following steps.

- Define a mission profile;
- Perform an electro-thermal simulation to estimate wear-out failure lifetime;
- Validate electro-thermal simulation with experimental setup;
- Account for cosmic ray induced random failures;
- Execute a Monte carlo analysis to account for statistical variation of component parameters.

The details of the SG system used in this work was discussed as an alternative for existing 3 stage synchronous generators [35]. The system was designed to supply starting torque to the main aircraft turbine during start-up. Once the main turbine reaches operating speed, the SG system acts as a generator and supplies power to the aircraft main electrical bus. The key parameters of the SG system are listed in Table 1 [36].

In [35], the SG drive converter was designed for a system voltage of 270 V and was realized using a 3L-NPC Si IGBT converter. In this work, 3 system voltage levels - 270 V, 540 V and 810 V are modelled, with 2 L and 3L-NPC topology at each voltage level. An additional simulation case is included at 810 V system voltage for 2 L converter with SiC devices bringing total number of analysed cases to 7. The device sizing and selection of all 7 cases are summarised in Appendix VII.

The motor parameters, such as the back EMF constant and the dq axes inductances, are linearly scaled with DC link voltage. The maximum electrical frequency of drive system

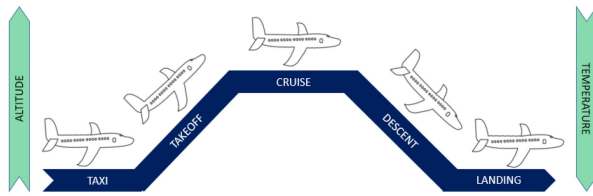


FIGURE 4. Flight stages of an aircraft.

TABLE 2. Flight Phase Duration

Flight Phase	Duration (mins)
Taxiing time	10
Cruise time	45
Climb/Descent time	Based on climb rate

TABLE 3. Climb/descent Rate of Aircraft

Altitude Range (feet)	Climb Rate (ft/min)
0-15,000	2,400
15,000-30,000	1,500
30,000-24,000	-1,000
24,000-10,000	-3,000
10,000-0	-2,000

is 1.6 kHz. The switching frequency is chosen as 20 kHz and 10 kHz for the 2 L and 3L-NPC converters respectively.

A. MISSION PROFILE OF SG SYSTEM

A mission profile is the defined operating conditions of a system which includes internal parameters (power, voltage, speed etc) and external parameters (ambient temperature, humidity, altitude etc). Hence, a mission profile quantifies the total amount of stress applied on a system during operation. The reliability analysis requires altitude, ambient temperature and output power in order to estimate stresses experienced by drive converter.

The following assumptions are made to generate a mission profile for a short haul aircraft.

- The flight time at cruise altitude is approximatively 1 h;
- Cruising altitude is fixed at 30 000 ft (9144 m);
- Total flight duration accounting for flight preparation, taxi, take-off, landing etc. is equal to 1 h 40 minutes;
- The same aircraft is modelled to operate 6 short haul flights a day.

A summary of the flight stages are illustrated in Fig. 4, while the simulated durations of each flight phase are summarised in Table 2.

The climb/descent rates of commercial airlines are typically widely variable and thus are not readily available in literature. Hence, reasonable assumptions are made for the case studies as detailed Table 3.

The ambient temperature profile during flight is generated from atmospheric models. According to US standard atmosphere 1976 [37], the thermal gradient in the lower atmosphere up to 36 000 feet (11000 m) is -6.5 °C/km. Monthly average ground temperature data of London for the period Aug 2018 till July 2019 is obtained from NCEP [38].

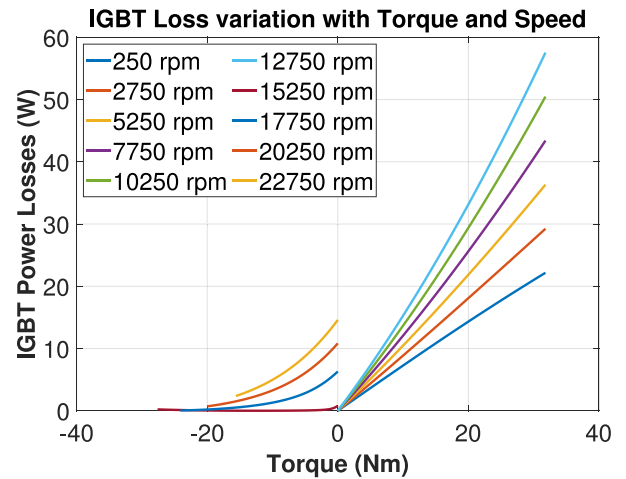


FIGURE 5. Outer IGBT loss profile with 540 V system voltage.

The output power requirement of the SG system is provided in [35]. During the start-up phase, the SG works in motoring mode, while for the cruising phase, the SG operates in generation mode at 90% of rated output power (i.e., 40 kW) and 18000 rpm. To account for operational variations during cruise conditions, 5% random variation in both output power and operating speed is modelled.

B. ELECTRO-THERMAL SIMULATION

The simulation model is setup in Matlab as a two-step model. In the first (computationally intensive) step, power losses of semiconductors, output current, power factor, thermal cycles of semiconductors at fundamental electrical frequency etc are pre-calculated and stored in a 3D lookup table for a range of machine speeds and output torque. Flux weakening is also included for operation beyond base speed. This database enables fast estimation of reliability figures at different mission profiles. A simplification is performed in thermal simulation by assuming loss figures at a junction temperature of 125 °C which is a conservative approach to reliability modelling [39].

The pre-estimated power loss profile for the outer IGBT of the 3L-NPC converter operating at 540 V is shown in Fig. 5. It can be observed that losses during generation mode (torque is negative) are very low as the outer IGBTs are rarely conducting current.

In the second step, a specific mission profile is simulated including atmospheric model to account for ambient temperature and altitude profile. The ambient temperature profile/altitude profile during a typical flight for one simulation run is reported in Fig. 6. Junction temperature swings at high frequency is not displayed as they follow the sinusoidal heating and cooling pattern as shown in [39]. Furthermore, high frequency thermal cycling is not a major contributor to IGBT wear-out as shown in Section. III-D.

The average power losses of semiconductors are defined from the 3D lookup table generated in the first step model. Combining the above variables in a modified foster thermal

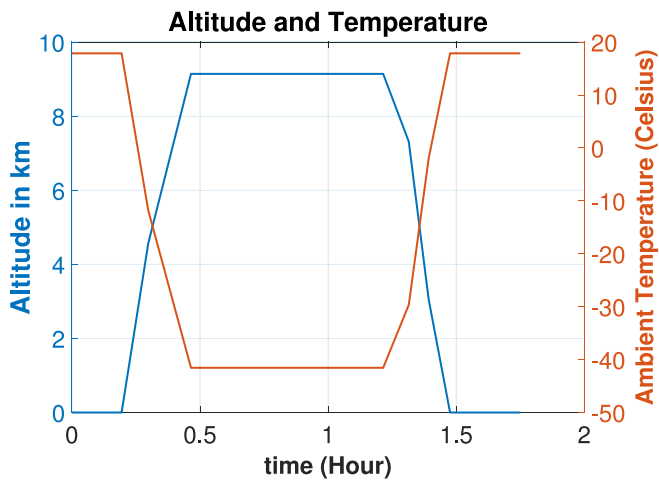


FIGURE 6. Altitude and temperature variation during flight.

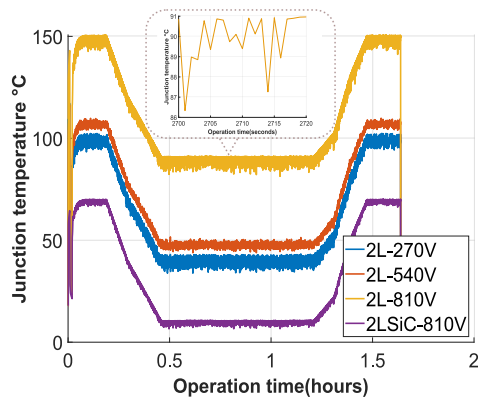


FIGURE 7. IGBT junction temperature variation.

simulation network [21], the medium frequency (duration of minutes to hours) junction temperature profile for semiconductors is obtained. Fundamental frequency thermal cycles are directly looked up from the lookup table. Junction temperature variation due to medium frequency cycles for 2 L converters at various system voltages is shown in Fig. 7. The effect of speed and power variations in steady state operation can be seen during cruise period. The thermal interface material (TIM) is modelled with a thermal impedance of 0.07 K/W. Heatsink to ambient thermal impedance is modelled with a thermal resistance of 0.1 K/W (0.2 K/W in the case of SiC converter) and the heat capacity of 1 kg of Aluminium (900 J/K).

The RMS current through the DC link capacitors is required to estimate the thermal stress applied on capacitors. The DC link capacitor rms current is evaluated as reported in literature for 2 L converter topology [40] and 3L-NPC topology [41]. The necessary variables for rms current calculation is also available in the lookup table. RMS current and ESR of capacitor is combined to generate power loss profile of the capacitors. The power losses are translated to a hot spot temperature by a simple thermal resistance model. The capacitor bulk temperature profile of 2 L converters are given in Fig. 8.

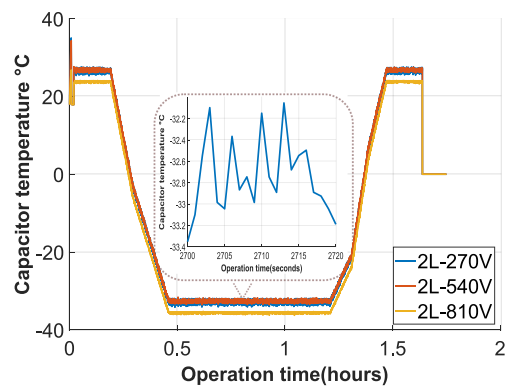


FIGURE 8. Capacitor temperature variation.

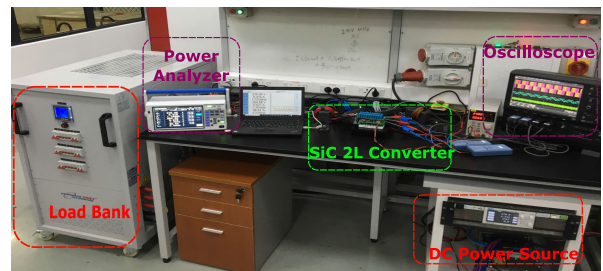


FIGURE 9. Test setup for SiC inverter power loss verification.

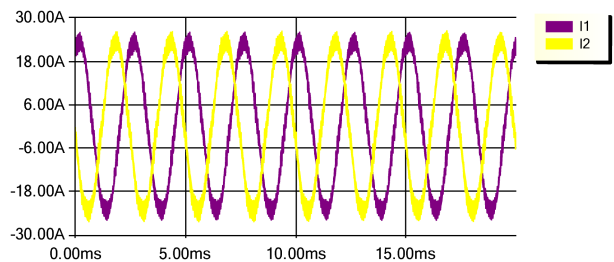


FIGURE 10. Phase A and B current output waveform at highest test load - 270 V 19 A DC input.

C. EXPERIMENTAL VALIDATION OF POWER LOSS ESTIMATION

The power losses in a 2 L SiC converter prototype are experimentally measured to validate loss estimation. The test setup is depicted in Fig. 9.

The setup consists of a DC power source, an RL load with an inductance of 0.5 mH and a variable resistor bank, Hioki PW3390 power analyzer and prototype SiC inverter. CCS050M12CM2 SiC power module from CREE rated at 1.2 kV and 87 A is used while the DC link is composed of 20 capacitors from TDK Epcos (B32652A4474J000) rated at 470 nF, 400 V. The output fundamental frequency is set to 400 Hz with a DC link voltage of 270 V. The output current waveform in two output phases at highest load power is shown in Fig. 10.

In the test frequency range, the power meter has an error margin of 0.1% maximum scale. The voltage and current measurements range for input and output power are set as

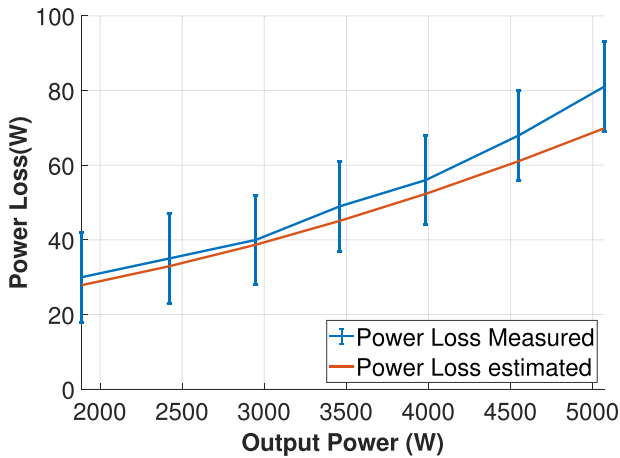


FIGURE 11. Power loss estimation versus measured loss.

300 V and 20 A respectively. Hence, the errors in both power and loss measurements are 6 W (0.1% of 6000 W) and 12 W respectively.

The measured and estimated power losses of the SiC inverter are plotted in Fig. 11. Datasheet values for typical power module was used for loss estimation which introduces an error considering the particular module under test. It is not practical to characterise each device especially mass produced commercial modules. Hence the error observed in power loss validation is considered acceptable as it is the industry norm. However, a further analysis is performed to bring out the dominance of cosmic ray failures on system reliability of aerospace converters even if wear out failures are under estimated due to statistical variation of device parameters. In Section III-D, the reliability estimates are recalculated with 20% higher losses, in order to account for potential errors in power losses modelling and how these affect the system reliability predictions (i.e., sensitivity evaluation).

D. WEAR-OUT FAILURE LIFETIME ESTIMATES

The stress profiles evaluated in Subsection III-B is applied to lifetime models introduced in Section II to obtain lifetime estimates for both semiconductors and capacitors. In the case of semiconductors, a rainflow cycle counting algorithm is employed to generate thermal cycle data as shown in Fig. 2.

Bayerer model specifies the range of t_{on} parameter as 1 to 15 seconds. Infineon published an extension method, [42], as summarized in (3).

$$\frac{N_{cyc}(t_{on})}{N_{cyc}(1.5s)} = \left(\frac{t_{on}}{1.5s} \right)^{-0.3}, 0.1s < t_{on} < 60s \quad (3)$$

In order to account for the thermal cycling time, t_{on} , appropriately in IGBT lifetime model (1), the thermal cycles are separated into three different time scales - sub second cycles (below 0.1 s) are classified as drive fundamental frequency cycles, thermal cycles of duration 0.1 s to 60 s are classified as fast thermal cycles and above 60 seconds are classified as slow cycles. The Bayerer model with the extension proposed by

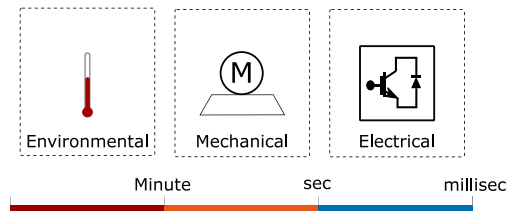


FIGURE 12. Junction thermal cycle classification of power modules.

infineon is only valid in the fast thermal cycles range. Thermal cycles and their origins are classified in Fig. 12.

The fundamental frequency component cycles are below the lower bound of the lifetime model validity. The contribution from those thermal cycles are very low as the power modules are sized to handle those fluctuations. The lifetime model predicts the same, even though caution must be exercised as it is outside the validity range. The slow thermal cycles pose a different challenge. They are smaller in number but cause the most amount of damage. The lifetime model cannot simply be extended as shown by ABB in [43]. In a prior work on wind converter reliability assessment, the ABB HiPak lifetime data was directly applied to quantify lifetime consumption due to long thermal cycles [11]. A closely related but different approach is adopted in this work.

The coefficient term of t_{on} in (1), β_3 is estimated using the lifetime figures published in [43]. The estimated coefficient termed $\beta_3(slow)$ is utilized to account for thermal stress due to long thermal cycles.

Lifetime estimates of semiconductors and capacitors without accounting for statistical variations for the 7 cases are listed in Table 4. Sub-zero ambient temperature at aircraft cruising altitudes coupled with reduced voltage stress, result in very high predicted lifetime for capacitors. The lifetime model for capacitors is saturated to a constant failure rate model when capacitor hotspot temperature is below 25 °C as recommended in IEC 61 709. The high predicted lifetime of capacitors indicate that thermal stress is not a lifetime consuming factor for capacitors under this mission profile. As listed in [44], further to applied voltage and hot-spot temperature, humidity is another stressor consuming lifetime of MPPF. Lifetime model utilized accounts for voltage and temperature induced stresses, humidity related failure modes could dominate in this particular case. Humidity induced lifetime consumption has been not considered in this work due to the following reasons - assumed hermetic sealing of capacitors, and low humidity conditions inside fuselage. It can be concluded that capacitors would not be the reliability bottleneck for aviation power electronic converters.

BVR is also included to show switch blocking capability utilization which would be utilized for cosmic ray failure rate estimation.

The revised lifetime estimates of semiconductors and capacitors accounting for 20% higher power losses are listed in Table 5. Comparing the lifetime predictions of Tables 4 and 5, the very strong impact on lifetime prediction due to loss

TABLE 4. Predicted Lifetime Values

DC Link Voltage	2L			3L			
	S1	Capacitor	BVR	S1	S2	Capacitor	BVR
270V	17.5 years	2461 years	0.46	56 years	38 years	6666 years	0.23
540V	9.8 years	1892 years	0.5	230 years	196 years	1284 years	0.46
810V	2.8 years	1533 years	0.74	309 years	304 years	1559 years	0.69
810V(SiC)*	96.9 years	1533 years	0.74	-	-	-	-
810V(SiC)**	71.8 years	1533 years	0.74	-	-	-	-

*Lifetime parameters in [16] utilized.**SiC Lifetime parameters extracted from [19] utilized.

TABLE 5. Lifetime Estimates With 20% Higher Losses

DC Link Voltage	2L		3L		
	S1	Capacitor	S1	S2	Capacitor
270V	8 years	2443 years	31 years	16 years	6310 years
540V	4.5 years	1876 years	170 years	136 years	922 years
810V	1.3 years	1533 years	231 years	230 years	1432 years
810V(SiC)*	60 years	1533 years	-	-	-
810V(SiC)**	42.8 years	1533 years	-	-	-

TABLE 6. Cosmic Ray Failure Rate Per Switch

	2L	3L
BVR	0.74	0.69
FIT rate/cm ² (Reference)	200	0.1
FIT rate/cm ² (Cruising)	26000	13
Die area (cm ²)	1.42	0.76
FIT rate Switch	36920	9.9

estimation error is evident. In practical reliability estimates, such statistical parameter deviations are accounted for by a Monte Carlo simulation to estimate system reliability over the population of such systems.

E. COSMIC RAY FAILURE RATE ESTIMATION

Experimental results in [29] highlight that Si IGBTs suffer from cosmic ray failures above 60% BVR, while the impact on SiC devices is negligible below 80% BVR. Cosmic ray failures are strongly dependent on switch voltage rating and device construction. The above observations are valid for switch voltage ratings up to 1200 V. The values could also be confirmed from the guide on cosmic ray failures from Semikron [23]. From Table 4, it is concluded that cosmic ray failure is only of concern for 2 L and 3L-NPC Si IGBT based converters operating at 810 V. Cosmic ray failure rate is tabulated and listed in Table 6 based on experimental FIT rates (number of failure per 1 billion hours) at estimated BVR of devices from [29] scaled to account for increased neutron flux intensity at altitude. Neutron flux intensity at 30 000 ft is 130 times higher than at reference conditions [27].

FIT rates listed in Table 6 are valid for a semiconductor during blocking mode. Due to modulation, scaling factors corresponding to percentage of time spent in blocking mode are applied for the switches:

- 50% for the devices in 2 L converter;
- 75% for the outer switches in 3L-NPC;
- 25% for the inner switches in 3L-NPC.

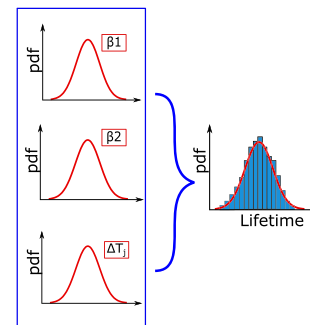


FIGURE 13. Monte Carlo Analysis with variation in lifetime parameters and thermal simulation results of IGBT.

Approximating the time at cruising altitude to be 1 h for every flight, cumulative failure rate caused by cosmic rays is:

- 2 L converter - 24.3% /year;
- 3L-NPC converter - 0.0013% /year.

Hence at 810 V, designing with 1200 V devices for a 2 L converter is simply not an option for aerospace converters. The failure rate of 3L-NPC converter due to cosmic ray failures, albeit smaller than that of 2 L converter, is still significant for the overall converter reliability, as discussed in Section IV.

IV. RELIABILITY RESULTS AND DISCUSSION

Estimated lifetimes in Section III-D do not account for statistical parameter variations of the converter components. In order to obtain time dependent reliability of converter system, a Monte Carlo simulation is carried out. The resultant reliability in time figures of individual components are combined together using reliability block diagram method to predict the converter reliability at system level.

A. MONTE CARLO SIMULATION FOR WEAR-OUT FAILURES

The Monte Carlo methodology applied in this work for semiconductors is described in [20] and for capacitors, is described in [45]. A virtual thermal swing, which would result in an equivalent amount of damage caused by the mission profile, is derived for semiconductors. This approach needs to be expanded if thermal heating time, i.e., ton, is also accounted for in lifetime model [46]. In the case of capacitors, a virtual hot spot temperature is estimated which corresponds to total damage imposed by mission profile. This is an established procedure based on reliability physics [47].

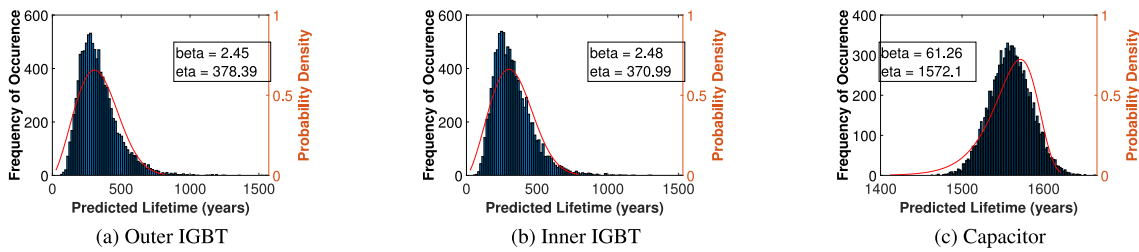


FIGURE 14. Monte Carlo simulation results for 3LNPC converter at 810 V.

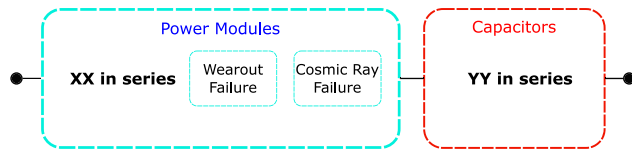


FIGURE 15. Reliability block diagram.

Once virtual effective stress values are determined, a Monte Carlo simulation is carried out assuming a 5% variation in all parameters of lifetime model as well as effective stress value [17]. A graphical overview of the Monte Carlo process highlighting the variation of parameters in the lifetime model is given in Fig. 13.

In the case of capacitors, only the lifetime value reported at nominal conditions is varied as failure model saturates to a constant failure mode due to low hotspot temperature. Monte Carlo simulation results showing wear-out failure reliability of sub components of 3L-NPC converter with DC link voltage of 810 V is provided in Fig. 14.

B. RELIABILITY BLOCK DIAGRAM METHOD

The reliability figures derived in Subsections III-E and IV-A are combined using the RBD method to estimate overall converter reliability. As no redundancy is factored in the converter design, the failure of a single component leads to the whole converter failing. The above assumption is held valid to develop RBD for all 7 cases. A reference RBD is illustrated in Fig. 15.

C. RELIABILITY FIGURES FROM CASE STUDY

The RBD based converter reliability for all cases is provided in Fig. 16.

The following conclusions could be drawn:

- At low system voltages (up to 270 V), Si based 2 L and 3L-NPC have similar reliability, with 2 L providing higher reliability;
- Above 540 V, 3L-NPC is able to achieve higher system reliability;
- Above 810 V, 2 L Si is not an option due to the very low system reliability. On the other hand, 2 L SiC outperforms 3L-NPC in terms of reliability albeit only in the initial years of operation. The wear-out reliability of SiC converters are easier to improve by paralleling modules

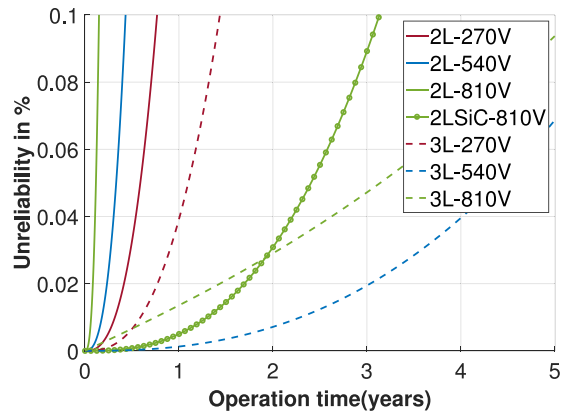


FIGURE 16. Reliability comparison of case study.

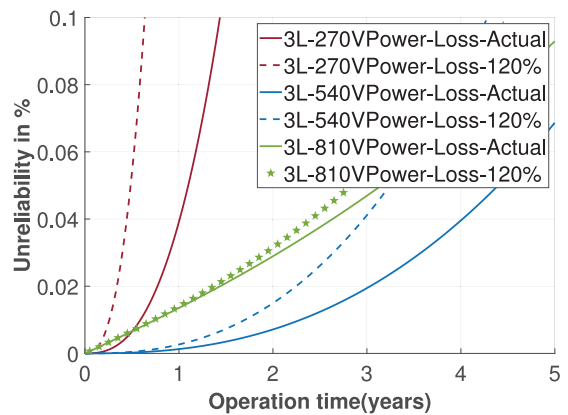


FIGURE 17. Reliability comparison of 3L-NPC topology with power loss variation.

as they are inherently more robust against cosmic ray failures.

The impact of power loss estimation errors on component lifetimes was presented in Table 5. In Fig. 17, the reliability of the 3L-NPC topology at the modelled system voltages is plotted along with estimated reliability considering 20% higher power losses. Considering 270 V and 540 V, the overall reliability is lower at higher power losses as expected. At those system voltages, the dominant failure mode is wear-out failure as BVR for switches is sufficiently low. An obvious choice to improve converter reliability at those voltage levels is higher current derating of sub-components.

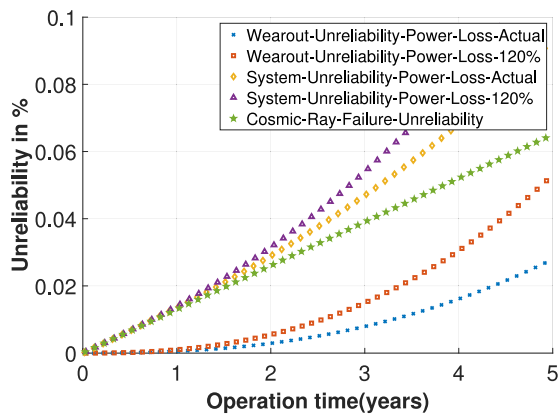


FIGURE 18. Reliability sub-components of 3L-NPC @ 810 V.

TABLE 7. Device/topology Selection Guide Considering Reliability

	2L	3L-NPC	2L-SiC
270V	✓	✓	-
540V	✓	✓✓	-
810V	XX	✓	✓✓

In order to explain the lower reliability performance of 3L-NPC converter at 810 V, system unreliability along with contribution from various failure modes to unreliability are plotted in Fig. 18 to identify the reliability bottleneck. Cosmic ray failure rate is assumed to be unchanged due to loss variation by ignoring the impact of junction temperature. System unreliability contribution due to wear-out of semiconductors and capacitors show a strong dependency to modelled losses. In spite of that, overall system unreliability is unchanged as cosmic ray failures are the dominant failure mechanism.

This result highlights the necessity for fault tolerance of high voltage converters based on Si IGBTs as dominant failure mode switches to cosmic ray failures (constant failure rate) instead of wear-out failures. Designers of future kV class aerospace power converters, must factor in tolerance against cosmic ray failure (sufficient voltage derating) along with fault tolerance as key design requirements. Designs with Si IGBTs for high voltage converters should derate the semiconductors for current as well as voltage to mitigate against wear-out failures and cosmic ray failures. Selection of higher current rated devices of same voltage rating would enhance wear-out failure performance at the expense of higher cosmic ray failure rate due to larger device surface area. A summary is provided in Table. 7 to assist system designer in making appropriate choices for devices/topologies at various voltage levels.

V. CONCLUSIONS

Extending the existing lifetime models to aerospace conditions, aerospace drive converter reliability for a steady power output system has been presented. It has been demonstrated that aerospace mission profile lies outside the validity range of widely accepted lifetime models of power electronic components - especially in the case of film capacitors and SiC

modules. New research is necessary to identify lifetime models valid in aerospace conditions. Simulated stress profiles indicate that at higher voltage levels, major failure mode for power electronics shifts from wear-out to cosmic ray induced random failures, mandating the adoption of multilevel topologies. At higher voltage levels the reliability limit is dictated by cosmic ray failure. Hence the reduced die area, wide bandgap and consequent higher tolerance to cosmic ray failures of SiC devices make them ideal candidate for power converters operated at altitude.

**APPENDIX A
COMPONENT SIZING**

TABLE 8. DC Link Capacitance for 2 L Topology

DC Link Voltage	Estimated Capacitance	Manufacturer Part number	Device Rating	Number of Caps
270V	684 uF	B32778J4487K000	480 uF, 450V	2
540V	171 uF	B32778G8107000	100 uF, 800V	2
810V	76 uF	B32778J0207K000	200 uF, 1100V	1

TABLE 9. Semiconductor Selection for 2 L Topology

DC Link Voltage	Manufacturer Part number	Device Rating	Die Area
270V	SKM400GB07E3	650V-400A	1.99cm ²
540V	SKM200GB12V	1200V-200A	1.93cm ²
810V	SKM150GB12T4	1200V-150A	1.42cm ²
810V	CAS120M12BM2	1200V-120A	-

TABLE 10. DC Link Capacitance for 3L-NPC Topology

DC Link Voltage	Estimated Capacitance	Manufacturer Part number	Device Rating	Number of Caps
270V	684 uF	B32778J4487K000	480 uF, 450V	6
540V	171 uF	B32778J4487K000	480 uF, 450V	2
810V	76 uF	B32778J5117K000	110 uF, 540V	4

TABLE 11. Semiconductor Selection for 3L Topology

DC Link Voltage	Manufacturer Part number	Device Rating	Die Area
270V	SEMiX405MLI07E4	650V-400A	1.99cm ²
540V	SEMiX205MLI07E4	650V-200A	0.99cm ²
810V	SEMiX155MLI07E4	650V-150A	0.76cm ²

ACKNOWLEDGMENT

The authors would like to mention that one of the co-authors and the initiator of this research work, Dr. Alessandro Costabeber passed away recently. The authors would like to acknowledge his immense contribution in particular to this work and overall to our research group. The authors dedicate this work to his memory.

REFERENCES

[1] E. H. L. G. On aviation research, flightpath 2050 Europe’s vision for aviation, European Commission, 2011.

- [2] IATA, DLR, and G. I. of Technology, IATA TECHNOLOGY ROADMAP 2013. Int. Air Transport Assoc., 2013.
- [3] M. Lukic, P. Giangrande, A. Hebala, S. Nuzzo, and M. Galea, "Review, challenges and future developments of electric taxiing systems," *IEEE Trans. Transport. Electric.*, vol. 5, no. 4, pp. 1441–1457, Dec. 2019.
- [4] V. Madonna, P. Giangrande, and M. Galea, "Electrical power generation in aircraft: Review, challenges, and opportunities," *IEEE Trans. Transport. Electric.*, vol. 4, no. 3, pp. 646–659, Sep. 2018.
- [5] G. Buticchi, S. Bozhko, M. Liserre, P. Wheeler, and K. Al-Haddad, "On-board microgrids for the more electric aircraft-technology review," *IEEE Trans. Ind. Electron.*, vol. 66, no. 7, pp. 5588–5599, Jul. 2019.
- [6] H. Chung, H. Wang, F. Blaabjerg, and M. Pecht, Reliability of Power Electronic Converter Systems, ser. Energy Engineering. Institution of Engineering and Technology, 2015. [Online]. Available: <https://books.google.co.uk/books?id=Ix4WrgEACAAJ>
- [7] M. Galea, P. Giangrande, V. Madonna, and G. Buticchi, "Reliability-oriented design of electrical machines: The design process for machines' insulation systems must evolve," *IEEE Ind. Electron. Mag.*, vol. 14, no. 1, pp. 20–28, Mar. 2020.
- [8] S. Yang, A. Bryant, P. Mawby, D. Xiang, L. Ran, and P. Tavner, "Industry-based survey of reliability in power electronic converters," in *Proc. IEEE Energy Convers. Congr. Expo.*, 2009, pp. 3151–3157.
- [9] X. Perpiñá, J. Serviere, L. Navarro, M. Mermet-Guyennet, M. Velvehí, and X. Jordá, Reliability and Lifetime Prediction for IGBT Modules in Railway Traction Chains. INTECH Open Access Publisher, 2012. [Online]. Available: <https://books.google.co.uk/books?id=LkLYoAEACAAJ>
- [10] D. Hirschmann, D. Tissen, S. Schroder, and R. W. D. Doncker, "Reliability prediction for inverters in hybrid electrical vehicles," *IEEE Trans. Power Electron.*, vol. 22, no. 6, pp. 2511–2517, Nov. 2007.
- [11] K. Ma, M. Liserre, F. Blaabjerg, and T. Kerekes, "Thermal loading and lifetime estimation for power device considering mission profiles in wind power converter," *IEEE Trans. Power Electron.*, vol. 30, no. 2, pp. 590–602, Feb. 2015.
- [12] M. H. M. Sathik, S. Prasanth, F. Sasongko, and J. Pou, "Lifetime estimation of off-the-shelf aerospace power converters," *IEEE Aerosp. Electron. Syst. Mag.*, vol. 33, no. 12, pp. 26–38, Dec. 2018.
- [13] D. C. Loder, A. Bollman, and M. J. Armstrong, "Turbo-electric distributed aircraft propulsion: Microgrid architecture and evaluation for eco-150," in *Proc. IEEE Transp. Electric. Conf. Expo.*, Jun. 2018, pp. 550–557.
- [14] J. F. Ziegler, "Terrestrial cosmic rays," *IBM J. Res. Dev.*, vol. 40, no. 1, pp. 19–39, Jan. 1996.
- [15] U. Scheuermann and M. Junghaenel, "Limitation of power module lifetime derived from active power cycling tests," in *Proc. 10th Int. Conf. Integr. Power Electron. Syst.*, Mar. 2018, pp. 1–10.
- [16] A. Wintrich, U. Nicolai, W. Tursky, and T. Reimann, *Application Manual Power Semiconductors, SEMIKRON International GmbH*, 2015.
- [17] D. Zhou, H. Wang, and F. Blaabjerg, "Mission profile based system-level reliability analysis of DC/DC converters for a backup power application," *IEEE Trans. Power Electron.*, vol. 33, no. 9, pp. 8030–8039, Sep. 2018.
- [18] R. Bayerer, T. Herrmann, T. Licht, J. Lutz, and M. Feller, "Model for power cycling lifetime of IGBT modules - Various factors influencing lifetime," in *Proc. 5th Int. Conf. Integr. Power Electron. Syst.*, Mar. 2008, pp. 1–6.
- [19] B. Hu *et al.*, "Failure and reliability analysis of a SiC power module based on stress comparison to a Si device," *IEEE Trans. Device Mater. Rel.*, vol. 17, no. 4, pp. 727–737, Dec. 2017.
- [20] P. D. Reigosa, H. Wang, Y. Yang, and F. Blaabjerg, "Prediction of bond wire fatigue of IGBTs in a pv inverter under a long-term operation," *IEEE Trans. Power Electron.*, vol. 31, no. 10, pp. 7171–7182, Oct. 2016.
- [21] K. Ma, N. He, M. Liserre, and F. Blaabjerg, "Frequency-domain thermal modeling and characterization of power semiconductor devices," *IEEE Trans. Power Electron.*, vol. 31, no. 10, pp. 7183–7193, Oct. 2016.
- [22] U. Scheuermann and U. Schilling, "Impact of device technology on cosmic ray failures in power modules," *IET Power Electron.*, vol. 9, pp. 2027–2035, 2016, doi: [10.1049/iet-pel.2015.1003](https://doi.org/10.1049/iet-pel.2015.1003).
- [23] D. U. Schilling, Cosmic Ray Failures in Power Electronics, Application Note AN 17-003, Semikron GmbH, 2017.
- [24] G. Soelkner, "Ensuring the reliability of power electronic devices with regard to terrestrial cosmic radiation," *Microelectronics Reliability*, vol. 58, pp. 39–50, 2016, *reliability Issues Power Electronics*. [Online]. Available: <https://www.sciencedirect.com/science/article/pii/S0026271415302663>
- [25] N. Kaminski, Failure rates of HiPak modules due to cosmic rays application note 5SYA 2042-02, ABB Switzerland Ltd, 2004.
- [26] I. E. Commission, Process Management for Avionics - Atmospheric Radiation Effects, International Electrotechnical Commission, 2017.
- [27] R. Edwards, C. Dyer, and E. Normand, "Technical standard for atmospheric radiation single event effects, (SEE) on avionics electronics," in *Proc. IEEE Radiation Effects Data Workshop* (IEEE Cat. No.04TH8774), Jul. 2004, pp. 1–5.
- [28] G. Consentino *et al.*, "Effects on power transistors of terrestrial cosmic rays: Study, experimental results and analysis," in *Proc. IEEE Appl. Power Electron. Conf. Expo.*, Mar. 2014, pp. 2582–2587.
- [29] C. Felgemacher, S. V. Araújo, P. Zacharias, K. Neemann, and A. Gruber, "Cosmic radiation ruggedness of Si and SiC power semiconductors," in *Proc. 28th Int. Symp. Power Semicond. Devices ICs*, Jun. 2016, pp. 51–54.
- [30] H. Wang and F. Blaabjerg, "Reliability of capacitors for dc-link applications in power electronic converters 2014; an overview," *IEEE Trans. Ind Appl.*, vol. 50, no. 5, pp. 3569–3578, Sep. 2014.
- [31] H. Wang and H. Wang, "Capacitive DC links in power electronic systems-reliability and circuit design," *Chin. J. Elect. Eng.*, vol. 4, no. 3, pp. 29–36, Sep. 2018.
- [32] R. Gally, "Metallized film capacitor lifetime evaluation and failure mode analysis," 2016, *arXiv:1607.01540*.
- [33] A. Hammoud and E. Overton, "Low temperature characterization of ceramic and film power capacitors," in *Proc. Conf. Elect. Insul. Dielectric Phenomena*, 1996, pp. 701–704.
- [34] I. E. Commission, Electric components - reliability - reference conditions for failure rates and stress models for conversion, international electrotechnical commission, 2017.
- [35] S. Bozhko *et al.*, "Development of aircraft electric starter-generator system based on active rectification technology," *IEEE Trans. Transport. Electric.*, vol. 4, no. 4, pp. 985–996, Dec. 2018.
- [36] F. Gao, S. Bozhko, Y. Seang Shen, and G. Asher, "Control design for PMM starter-generator operated in flux-weakening mode," in *Proc. 48th Int. Univ. Power Eng. Conf.*, Sep. 2013, pp. 1–6.
- [37] National Oceanic and Atmospheric Administration, National Aeronautics and Space Administration, US Air Force, "US Standard Atmosphere," 1976.
- [38] E. Kalnay *et al.*, "NCEP/NCAR 40-Year Reanalysis Project," Bulletin of the American Meteorological Society, vol. 77, no. 3, pp. 437–472, 1996. [Online]. Available: [https://doi.org/10.1175/1520-0477\(1996\)077<0437:TNYRP>2.0.CO;2](https://doi.org/10.1175/1520-0477(1996)077<0437:TNYRP>2.0.CO;2)
- [39] D. A. Wintrich, ECPE tutorial thermal engineering of power electronics systems 1 - first steps of a converter design, SEMIKRON Elektronik GmbH, Jul. 2018.
- [40] J. W. Kolar and S. D. Round, "Analytical calculation of the RMS current stress on the DC-link capacitor of voltage-PWM converter systems," *IEE Proc. - Elect. Power Appl.*, vol. 153, no. 4, pp. 535–543, Jul. 2006.
- [41] K. Gopalakrishnan, S. Janakiraman, S. Das, and G. Narayanan, "Analytical evaluation of DC capacitor RMS current and voltage ripple in neutral-point clamped inverters," *Sadhana - Acad. Proc. Eng. Sci.*, vol. 42, pp. 1–13, 05 2017, doi: [10.1007/s12046-017-0668-y](https://doi.org/10.1007/s12046-017-0668-y).
- [42] Infineon Technologies AG, "AN 2019-05: PC and TC Diagrams - Use of Power Cycling Curves for IGBT4," Infineon Technologies AG, 2019.
- [43] E. Özkol and S. Hartmann, Load-cycle capability of HiPak IGBT modules application note 5SYA 2043-04, ABB Switzerland Ltd, 2014.
- [44] H. Wang *et al.*, "Transitioning to physics-of-failure as a reliability driver in power electronics," *IEEE Trans. Emerg. Sel. Topics Power Electron.*, vol. 2, no. 1, pp. 97–114, Mar. 2014.
- [45] H. Wang, P. Davari, H. Wang, D. Kumar, F. Zare, and F. Blaabjerg, "Lifetime estimation of DC-link capacitors in adjustable speed drives under grid voltage unbalances," *IEEE Trans. Power Electron.*, vol. 34, no. 5, pp. 4064–4078, May. 2019.
- [46] K. Ma, U. Choi, and F. Blaabjerg, "Prediction and validation of wear-out reliability metrics for power semiconductor devices with mission profiles in motor drive application," *IEEE Trans. Power Electron.*, vol. 33, no. 11, pp. 9843–9853, Nov. 2018.
- [47] J. McPherson, *Reliability Physics and Engineering: Time-to-Failure Modeling*. Springer US, 2010. [Online]. Available: <https://books.google.co.uk/books?id=pXKZFEOZkWC>



JAYAKRISHNAN HARIKUMARAN received the B.Tech. degree in electronics and communication engineering from the National Institute of Technology Calicut, Kerala, India, in 2008 and M.S. degree in sustainable energy technology from the Delft University of Technology, Delft, Netherlands, in 2012.

He has worked with Texas Instruments (2008–2010), Twilight B.V (2012–2013) and Shell International B.V (2013–18) on various roles—semiconductor design, embedded systems engineering, industrial control systems and electrical engineering. Since 2018, he is a Marie-Curie doctoral Researcher with the Institute for Aerospace Technology, University of Nottingham, United Kingdom. His research interests include design for reliability of power converters, fault tolerant drive systems and digital controller implementation for power converters in DSP and FPGA.



PAOLO GIANGRANDE (Senior Member, IEEE) received the bachelor's (Hons.) and master's (Hons.) degrees in electrical engineering from the Politecnico of Bari in 2005 and 2008, respectively. He received the Ph.D. degree in electrical engineering from the Politecnico of Bari in 2011. Since 2012, he was a Research Fellow with the University of Nottingham (U.K.), within the Power Electronics, Machines and Control Group. In 2018, he was appointed Senior Research Fellow and he is currently head of the Accelerated Lifetime Testing

Laboratory with the Institute of Aerospace Technology, Nottingham. His main research interests include sensorless control of AC electric drives, design and testing of electromechanical actuators for aerospace, thermal management of high-performance electric drives and lifetime modeling of electrical machines.



GIAMPAOLO BUTICCHI (Senior Member, IEEE) received the master's degree in electronic engineering and the Ph.D degree in information technologies from the University of Parma, Italy, in 2009 and 2013, respectively. In 2012, he was a Visiting Researcher with The University of Nottingham, U.K. Between 2014 and 2017, he was a Postdoctoral Researcher, and a Guest Professor with the University of Kiel, Germany. During his stay in Germany, he was awarded with the Von Humboldt Postdoctoral Fellowship to carry out research related to fault tolerant topologies of smart transformers. In 2017, he was appointed as Associate Professor in Electrical Engineering, The University of Nottingham Ningbo China and as the Head of Power Electronics of the Nottingham Electrification Center. He was promoted to Professor in 2020. His research focuses on power electronics for renewable energy systems, smart transformer fed micro-grids and dc grids for the More Electric Aircraft. Dr. Buticchi is one of the advocates for DC distribution systems and multi-port power electronics onboard the future aircraft.

related to fault tolerant topologies of smart transformers. In 2017, he was appointed as Associate Professor in Electrical Engineering, The University of Nottingham Ningbo China and as the Head of Power Electronics of the Nottingham Electrification Center. He was promoted to Professor in 2020. His research focuses on power electronics for renewable energy systems, smart transformer fed micro-grids and dc grids for the More Electric Aircraft. Dr. Buticchi is one of the advocates for DC distribution systems and multi-port power electronics onboard the future aircraft.



ALESSANDRO COSTABEBER (Member, IEEE) received the master's degree (with Hons.) in electronic engineering and the Ph.D. degree in information engineering from the University of Padova, Padova, Italy, in 2008 and 2012, respectively, on energy efficient architectures and control techniques for the development of future residential microgrid.

In 2012, he started a two-year research fellowship with the University of Padova. In 2014, he joined the PEMC group, Department of Electrical and Electronic Engineering, University of Nottingham, Nottingham, U.K., as a Lecturer in Power Electronics. Dr. Costabeber was the recipient of the IEEE Joseph John Suozzi INTELEC Fellowship Award in power electronics in 2011.

He passed away recently and this work is dedicated to his memory.



GIOVANNI MIGLIAZZA received the master's degree in mechatronic engineering and the Ph.D. degree in industrial innovation engineering from the University of Modena and Reggio Emilia, Modena, Italy, in 2014 and 2020, respectively. He is currently a Senior Research Fellow with the University of Nottingham Ningbo China. He has authored or coauthored more than fifteen scientific papers and has received one industrial patent. His research interests include power electronics, converters, and electric drives.



PATRICK WHEELER (Fellow, IEEE) received the B.Eng. (Hons.) degree from the University of Bristol, U.K., in 1990. He received the Ph.D. degree in electrical engineering for his work on Matrix Converters from the University of Bristol, U.K., in 1994. In 1993, he moved to the University of Nottingham and worked as a Research Assistant with the Department of Electrical and Electronic Engineering. In 1996, he became a Lecturer in the Power Electronics, Machines and Control Group with the University of Nottingham, U.K. Since January 2008, he has been a Full Professor with the same Research Group. He was Head of the Department of Electrical and Electronic Engineering with the University of Nottingham from 2015 to 2018. He is currently the Head of the Power Electronics, Machines and Control Research Group, Global Director of the University of Nottingham's Institute of Aerospace Technology and was the Li Dak Sum Chair Professor in Electrical and Aerospace Engineering. He is a Vice President of the IEEE PELs and was an IEEE PELs Distinguished Lecturer from 2013 to 2017. He has authored or coauthored 750 academic publications in leading international conferences and journals.

He is currently the Head of the Power Electronics, Machines and Control Research Group, Global Director of the University of Nottingham's Institute of Aerospace Technology and was the Li Dak Sum Chair Professor in Electrical and Aerospace Engineering. He is a Vice President of the IEEE PELs and was an IEEE PELs Distinguished Lecturer from 2013 to 2017. He has authored or coauthored 750 academic publications in leading international conferences and journals.



VINCENZO MADONNA (Member, IEEE) received the Laurea Magistrale degree in electrical engineering from the University of Bologna, Italy, in 2016, and the Ph.D. degree in electrical machines design from the University of Nottingham, U.K., in 2020. In 2016, he joined the Institute for Aerospace Technology with the University of Nottingham, U.K. as a Marie Skłodowska-Curie Doctoral Fellow in reliability-oriented design of electrical machines for transportation. Throughout 2018, he was a Research Associate and Teaching

Assistant with the Key Laboratory of More Electric Aircraft of Zhejiang Province, Ningbo, China. He is currently a Research Fellow with the Propulsion Futures Beacon of Excellence with the University of Nottingham, U.K. He is authored or coauthored more than 40 scientific papers published in top academic journals and conference proceedings. His research interests include design, thermal management and lifetime prediction modeling of electrical machines.



MICHAEL GALEA (Senior Member, IEEE) received the Ph.D. degree in electrical machines design from the University of Nottingham, Nottingham, U.K., in 2013. He was appointed as a Lecturer in 2014, as an Associate Professor in 2018 and as a Professor in Electrical Machines and Drives in 2019, all with the University of Nottingham. He currently lectures in Electrical Machines and Drives and in Aerospace Systems Integration and manages a number of diverse projects and programmes related to the more/all electric aircraft, electrified propulsion, and associated fields. His main research interests include design and development of electrical machines and drives (classical and unconventional), reliability and lifetime degradation of electrical machines and the more electric aircraft. Michael is a Fellow of the Royal Aeronautical Society. Michael also is an Associate Editor for the IEEE TRANSACTIONS ON INDUSTRIAL ELECTRONICS and for the *IET Electrical Systems in Transportation*.

He is currently the Head of the Power Electronics, Machines and Control Research Group, Global Director of the University of Nottingham's Institute of Aerospace Technology and was the Li Dak Sum Chair Professor in Electrical and Aerospace Engineering. He is a Vice President of the IEEE PELs and was an IEEE PELs Distinguished Lecturer from 2013 to 2017. He has authored or coauthored 750 academic publications in leading international conferences and journals.